which we found to be predominant over the atomic signal as soon as soon as the laser intensity decreases below 1 GW/cm^2.

In conclusion we would like to emphasize that the validity of second-order perturbation theory is well verified for the two-photon ionization of cesium in the 460–540-nm wavelength range. The deep minimum in ionization cross section predicted by theory is clearly demonstrated in the present experiment and absolute values of σ_2 are found in satisfactory agreement with theoretical results. Finally, as far as the position and the depth of the σ_2 valley are concerned, our experimental measurements are sufficiently accurate to be useful to test the accuracy of the different calculational models proposed in the literature.[2]

Moreover, it is obvious from Fig. 3 that the "laser-bandwidth effects" predicted in Ref. 6 are not observed in this experiment, although our laser line is five times wider than the line of the argon-ion laser used by GVW. Finally, with regard to the "time-dependent effects" of Ref. 5, we point out that under our experimental conditions the sudden approximation[13] does not apply since the laser-pulse rise time is orders of magnitude larger than the Rabi oscillations period $2\pi/$ δ, where δ is the detuning from the resonance $7P_{1/2}$ state.

[1]H. B. Bebb, Phys. Rev. 149, 26 (1966).

[2]M. R. Teague, P. Lambropoulos, D. Goodmanson, and D. W. Norcross, Phys. Rev. A 14, 1057 (1976).

[3]A. Rachman, G. Laplanche, and M. Jaouen, Phys. Lett. 68A, 433 (1978).

[4]E. H. A. Granneman and M. J. Van der Wiel, J. Phys. B 8, 1617 (1975).

[5]C. E. Theodosiou and L. Armstrong, Jr., J. Phys. B 12, L87 (1979).

[6]L. Armstrong, Jr., and J. H. Eberly, J. Phys. B 12, L291 (1979).

[7]M. Lapp and L. P. Harris, J. Quant. Spectrosc. Radiat. Transfer 6, 169 (1966).

[8]M. Klewer, M. J. M. Beerlage, E. H. A. Granneman, and M. J. Van der Wiel, J. Phys. B 10, L243 (1977).

[9]D. Normand and J. Morellec, to be published.

[10]B. Held, G. Mainfray, C. Manus, and J. Morellec, Phys. Rev. Lett. 28, 130 (1972).

[11]J. L. Debethune, Nuovo Cimento 12, 101 (1972).

[12]M. R. Cervenan, R. H. C. Chan, and N. R. Isenor, Can. J. Phys. 53, 1573 (1975).

[13]C. E. Theodosiou, L. Armstrong, Jr., M. Crance, and S. Feneuille, Phys. Rev. A 19, 766 (1979).

[14]T. B. Cook, F. B. Dunning, G. W. Foltz, and R. F. Stebbings, Phys. Rev. A 15, 1526 (1977).

Direct Inversion of Rotationally Inelastic Cross Sections: Determination of the Anisotropic Ne-D₂ Potential

R. B. Gerber and V. Buch

Department of Physical Chemistry, The Hebrew University of Jerusalem, Jerusalem, Israel

and

U. Buck, G. Maneke, and J. Schleusener

Max-Planck Institut für Strömungsforschung, 3400 Göttingen, Federal Republic of Germany

The anisotropic interaction potential for Ne-D_2 is determined by a direct inversion method from the measured rotationally inelastic $j = 0 \rightarrow j = 2$ and elastic $j = 0 \rightarrow j = 0$ differential cross sections. The values obtained yield the repulsive part of the interaction in the range 2.43 to 2.77 Å. This is the first inversion of inelastic scattering data. The method is restricted to weak inelastic systems. It is computationally simple, and involves only errors of ∼ 5% in the inverted potential.

The purpose of this Letter is to present a first direct inversion of measured inelastic molecular cross sections, to yield the underlying intermolecular potential energy surfaces. For purely elastic atom-atom scattering systems, direct inversion methods have been available for some time,[1,2] and have proved successful in avoiding the difficulties of trial-and-error fitting. The motivation to develop such methods for inelastic scattering stems from recent progress in molecu-

lar-beam scattering experiments, that made pos-
sible the measurement of rotationally state-se-
lected differential cross sections (dcs) for a num-
ber of systems.[3-8] The cross sections obtained
in these experiments contain information sensi-
tive to the anisotropic potential involved. Sys-
tems for which state-selected dcs were deter-
mined include Ne-HD,[4] He-HD,[5] HD-HD,[6] and D_2-
HD,[7] where the transitions measured were $j = 0$
$\rightarrow j' = 1$ and $j = 0 \rightarrow j' = 1$; and He-Na_2,[8] for which
transitions $j \rightarrow j'$ for several j values were ob-
tained. Very recently, an inversion method was
proposed for data consisting of such state-select-
ed elastic and inelastic cross sections,[9] but it
was tested only for artificial (simulated) data. In
the present Letter we apply the method to meas-
ured cross sections for Ne-D_2, and determine
the anisotropic potential for this system.

An optimal experimental system for the pur-
pose of the present inversion method would beam
$X + H_2$ (D_2) since for $X +$ HD systems the effect of
the anisotropic part of the potential is partly
masked by the influence of the mass asymmetry.[10]
Thus, the experimental results recently obtained
for the dcs of the $j = 0 \rightarrow j = 0$ and $j = 0 \rightarrow j' = 2$ tran-
sitions in D_2-Ne scattering at energy $E = 0.0849$
eV are used as input data.[11] Since the inversion
procedure requires data from the entire nonos-
cillatory region, the measurements which were
available only from 38° to 108° were extended in
the backward direction. The experiments were
carried out in a molecular beam machine[4] con-
sisting of two colliding nozzle beams, a sensi-
tive mass-spectrometer detector operating at
pressures lower than 10^{-10} mbar, and a pseudo-
random-chopping technique for analyzing the
flight times of the scattered particles. Compared
with the published experimental arrangement,
the pumping facilities were improved to produce
nozzle beams at stagnation pressures up to 195
bars from nozzles of 10 μm diam. In this way
the velocity resolution ($\Delta v/v \approx 0.04$), the scat-
tered intensity, and the fraction of molecules in
$j = 0$ (0.89) could be considerably improved. The
data for the cross-section ratio ($j = 0 \rightarrow j' = 2$)/
($j = 0 \rightarrow j' = 0$) are given in Table I. These values
are obtained by carefully fitting the measured
time-of-flight distributions with calculated func-
tions which account for all the experimental aver-
aging effects and by transforming these data to
the center-of-mass (c.m.) system.[10] In fact, the
final values given in Table I are averaged over
two data sets measured for orthodeuterium and
normal deuterium, which are in good agreement

TABLE I. Input data.

θ	$\sigma_{0 \rightarrow 2}/\sigma_{0 \rightarrow 0}$	Uncertainty
37°	0.035	± 0.011
51°	0.056	± 0.010
66°	0.079	± 0.011
80°	0.112	± 0.011
94°	0.154	± 0.012
108°	0.193	± 0.013
136°	0.297	± 0.040
150°	0.316	± 0.045
163°	0.352	± 0.055

within their experimental errors. The errors
are estimated from the scatter of the data and
the fit procedure to the spectra. Since the c.m.
angles for the elastic and the inelastic transition
are very close, only the average angle is given.

For low-anisotropy, mass-symmetric systems
the potential surface can be represented to suffi-
cient accuracy in the form $V(r, \gamma) = V_0(r) + V_2(r)$
$\times P_2(\cos \gamma)$, where r is the distance between the
atom and the molecular c.m., and γ is the angle
between the distance vector and the molecular
axis. The inversion procedure deals then with
the determination of the unknown functions $V_0(r)$
and $V_2(r)$ from the measured dcs $\sigma_{j \rightarrow j'}(\theta)$ (θ is
the c.m. scattering angle) for $j = 0$ and $j' = 0, 2$.
The assumptions involved in the method are the
following[9]: (1) Restriction to a two-state frame-
work ($j = 0, 2$) is made. (2) The relative angular
momentum of the collision partners $\hbar l$ is as-
sumed to be approximately conserved. (3) Inelas-
ticity is taken to be significant only for large-an-
gle scattering, corresponding to small-impact
collisions. For this angular range the cross sec-
tions are smooth, free of interference oscilla-
tions. A classical-limit approximation can then
be used, relating θ uniquely to a corresponding
angular momentum l value. (4) Restriction to low
anisotropy and moderate collision energies is
adopted, implying that the exponential distorted-
wave approximation[12] should be valid. A detailed
discussion of the validity of (1)–(4) for the sys-
tems studied here can be found in Ref. 9. In the
framework of the above assumptions it can be
shown that to a good approximation $V_0(r)$ is the
potential obtained if the total dcs $\sigma_{\text{tot}}(\theta) = \sigma_{0 \rightarrow 0}(\theta)$
$+ \sigma_{0 \rightarrow 2}(\theta)$ is inverted as in a purely elastic-scat-
tering problem. A suitable inversion method for
the elastic case is available,[2] and thus $V_0(r)$ can
be assumed known. In the present practical case
of Ne-D_2 a reliable $V_0(r)$ was available from a

simultaneous fit to the measured total differential cross section and the virial coefficient.[11] [$V_0(r)$ is shown in Fig. 2.]

The inversion of the anisotropic potential component $V_2(r)$ is done in a two-step scheme: From the $\sigma_{0\rightarrow j}(\theta)$ the S-matrix elements $S_{0j}(l)$ ($j = 0, 2$) are determined as a function of l; $V_2(r)$ is recovered from the $S_{0j}(l)$. These two steps reverse the two conceptual stages involved in the calculation of $\sigma_{0\rightarrow j}(\theta)$ when the potential is known. It is shown in (9) that under conditions (1)–(4) above, the $S_{0j}(l)$ are approximately given by

$$|S_{02}(l)|^2 = \sin^2[a(l)], \quad |S_{00}(l)|^2 = 1 - |S_{02}(l)|^2, \quad (1)$$

$$\tan^2[a(l_{av})] = \frac{\sigma_{0\rightarrow 2}(\theta)}{\sigma_{0\rightarrow 0}(\theta)} \frac{l_{av}}{l_0} \frac{|\theta_0'(l_0 + \frac{1}{2})|}{|\theta_{av}'(l_{av} + \frac{1}{2})|}, \quad (2)$$

where $\theta_{av}(l) = \frac{1}{2}[\theta_0(l) + \theta_2(l)]$, and $\theta_0(l)$, $\theta_2(l)$ denote the classical deflection functions calculated from the isotropic potential $V_0(r)$ at the two channel energies E_0, E_2, respectively. l_{av}, l_0 are defined as the solutions of

$$\theta_0(l_0 + \tfrac{1}{2}) = \theta; \quad \theta_{av}(l_{av} + \tfrac{1}{2}) = \theta. \quad (3)$$

The above equations hold only for angles beyond the diffraction-oscillation regime in the dcs which contain the most sensitive information on $V_2(r)$. In the present case, the l values obtained from the smooth range were $\theta \lesssim l \lesssim 26$. The $a(l)$ values extracted from the data of Table I by Eqs. (1)–(3) are shown in Fig. 1. The $a(l)$ can be shown to be distorted-wave integrals[9]:

$$a(l) = C \int_0^\infty \psi_{0l}^{(0)}(r) V_2(r) \psi_{2l}^{(0)}(r)\, dr, \quad (4)$$

where C is a constant and $\psi_{jl}^{(0)}$, $j = 0, 2$, are the two zero-order channel-wave functions calculated from $V_0(r)$ only. Figure 1 shows the comparison between the $a(l)$'s extracted directly from the data, and those reproduced from the inverted

$V_2(r)$ obtained below. The excellent agreement obtained indicates consistency of the inversion results.

The extraction of $V_2(r)$ from the $a(l)$ is done by one of the variants of the peeling method[9,13]: The r space is divided into small intervals in each of which $V_2(r)$ is approximated by a linear function. It was shown[9] that each $a(l)$ is sensitive mainly to a contribution from a small r interval. By use of some estimate of $V_2(r)$, the segments into which r is divided can be chosen to correspond to the regions to which the various $a(l)$ are sensitive. The sensitivity ranges from all $a(l)$ available in the present example cover the domain 2.43–2.77 Å. The inversion procedure determines $V_2(r)$ in the range to which the data are sensitive. Previous knowledge is necessary of a rough estimate of $V_2(r)$ for large r, outside the above sensitivity range. (We used for large r the values from Tang and Toennies[14] that fit experiments sensitive to this regime.[15]) The peeling starts from $a(l)$ for the largest l available, using that quantity to determine the longest-range linear segment of $V_2(r)$.[13] The $a(l)$ for successively lower l are used to determine the interaction in shorter-range intervals.[9,13] The method derives explicit equations for the linear parameters of $V_2(r)$ in each segment and the inversion is there-
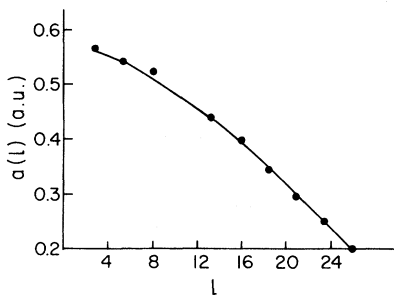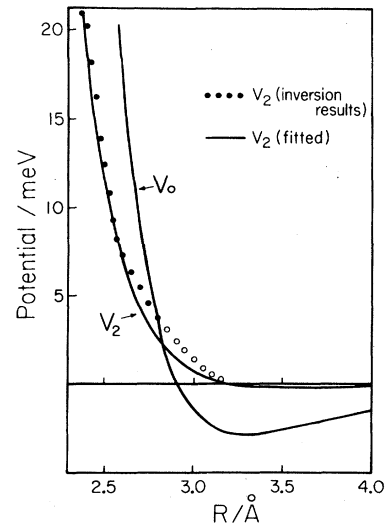
FIG. 1. The distorted-wave integrals $a(l)$ obtained by inversion of the experimental data. The solid line shows calculated values based on the potential derived by inversion.

FIG. 2. The anisotropic potential $V_2(R)$ for D_2-Ne obtained by the inversion of the data of Table I and the isotropic potential V_0 (Ref. 11). The dots mark the range of the potential based on the real data, whereas the open circles are extrapolated values. For comparison the $V_2(R)$ potential determined by a fit procedure (Ref. 11) is given.

fore direct.

Figure 2 shows the inverted potential, compared with results of a trial-and-error fitting effort[11] (coupled-channels calculations were used to calculate cross sections from the trial potentials). The agreement is excellent; the small deviation seen can be attributed to the limited flexibility of the potential function used for fitting (it could not reproduce the data points for the two smallest angles). The error in the results is expected to reflect mostly the experimental error in the data. It can therefore be estimated from Eqs. (2) and (4). It is of the order of 5% in the potential in the present case. A small additional error ($\sim 3\%$) could arise from the inaccuracy of using an assumed potential in the range of large r (to which the data are only slightly sensitive). Comparison of the inverted potential with the semiempirical model of Tang and Toennies[14] shows that the latter is more repulsive, typically by a few millielectronvolts (3 meV at 2.5 Å). The deviation is significant in view of the estimated error for the present results. The example of this Letter shows that the inversion method is easy to apply and reliable. It avoids the use of fitting procedures with repeated solution of complicated coupled-channels equations for trial potentials. It is an advantage of the method that it can be applied in its present form to a major class of experimentally accessible systems (e.g., $\chi + H_2, D_2$).

[1]U. Buck, Adv. Chem. Phys. 30, 314 (1975).

[2]R. B. Gerber, M. Shapiro, U. Buck, and J. Schleusener, Phys. Rev. Lett. 41, 236 (1978).

[3]M. Faubel and J. P. Toennies, Adv. At. Mol. Phys. 13, 229 (1977).

[4]U. Buck, F. Huisken, J. Schleusener, and H. Pauly, Phys. Rev. Lett. 38, 680 (1977).

[5]W. R. Gentry and C. F. Giese, J. Chem. Phys. 67, 5389 (1977).

[6]W. R. Gentry and C. F. Giese, Phys. Rev. Lett. 39, 1259 (1977).

[7]U. Buck, F. Huisken, and J. Schleusener, J. Chem. Phys. 68, 5654 (1978).

[8]K. Bergmann, R. Engelhardt, U. Hefter, and J. Witt, J. Chem. Phys. 71, 2726 (1979).

[9]R. B. Gerber, V. Buch, and U. Buck, to be published.

[10]U. Buck, F. Huisken, J. Schleusener, and J. Schafer, to be published.

[11]J. Andres, U. Buck, F. Huisken, J. Schleusener, and F. Torello, in Proceedings of the Eleventh International Conference on the Physics of Electronic and Atomic Collisions, Abstracts of Papers, edited by K. Takayanagi and N. Oda (Society of Atomic Collision Research, Kyoto, 1979).

[12]R. D. Levine, Mol. Phys. 22, 497 (1971).

[13]M. S. Child and R. B. Gerber, Mol. Phys. 38, 421 (1979).

[14]K. T. Tang and J. P. Toennies, J. Chem. Phys. 68, 5501 (1978).

[15]L. Zandee and J. Reuss, Chem. Phys. 68, 700 (1978).

Image Formation with Ultracold-Neutron Waves

Gisela Schütz and Albert Steyerl
Technische Universität München, D-8046 Garching, Germany

and

Walter Mampe
Institut Laue-Langevin, F-38042 Grenoble, France

Three-dimensional ultracold-neutron focusing by a total-reflecting concave Fresnel-zone mirror has been observed. In the neutron wavelength range from 60 to 80 nm, real-image formation was achieved up to a magnification of 6. The measured image positions, magnifications, and intensities agree with expectation. Within the instrumental resolution no image broadening due to diffuse scattering has been observed.

PACS numbers: 41.80.-y, 06.90.+v

Recently, two of the present authors have proposed[1] an achromatic optical device for image formation with ultracold neutrons (UCN's) in the wavelength range 60 nm $< \lambda <$ 80 nm. In principle, concave mirrors may be used for image formation with UCN's utilizing the property of total re-